Imaging analysis of 13 rare cases of renal collecting (Bellini) duct carcinoma patients in northern China: a case series and literature review.

Zhehao Lyu
the First Affiliated Hospital of Harbin Medical University
Lili Liu
the Second Affiliated Hospital of Harbin Medical University
Huimin Li
Inner Mongolia Autonomous Region People's Hospital
Haibo Wang
the Second Affiliated Hospital of Harbin Medical University
Qi Liu
the First Affiliated Hospital of Harbin Medical University
Tingting Chen
the Second Affiliated Hospital of Harbin Medical University
Meiling Xu
the Second Affiliated Hospital of Harbin Medical University
Lin Tian
the First Affiliated Hospital of Harbin Medical University
Peng Fu (fupeng0451@163.com)
the 1st affliated hospital of HMU https://orcid.org/0000-0002-9860-9150

Research article

Keywords: Collecting (Bellini) Duct Carcinoma, Kidney Neoplasms, Tomography Scanners, X-Ray Computed, Positron Emission Tomography Computed Tomography

Posted Date: October 28th, 2020

DOI: https://doi.org/10.21203/rs.3.rs-28998/v4

Version of Record: A version of this preprint was published on March 6th, 2021. See the published version at https://doi.org/10.1186/s12880-021-00574-8.

Abstract

Background: Collective duct carcinoma (CDC) is a highly malignant kidney tumor which is rare in clinical. We report our 12-year experience of Collecting (Bellini) duct carcinoma (CDC) and retrospectively analyzed patients and tumour characteristics, clinical manifestations, different imaging characteristics including CT, MRI and PET/CT.

Methods: From January 2007 to December 2019, we retrospectively examined all renal tumors and identifed 13 cases of CDC from 3 medical centers in the northern China. All 13 patients underwent CT scan, 8 of whom underwent dynamic enhanced CT scan, 2 underwent PET/CT scan and 1 underwent MRCP examination. The lesions were divided into nephritis type and mass type according to the morphology of the tumors.

Results: The study group included 10 men and 3 women, with an average age of 64.23±10.74 years old. Of these 13 patients, the main clinical manifestations include gross hematuria, flank pain or waist discomfort. The mean tumour size was 8.48 ± 2.48 cm. In this group of cases, 6 (46.2%) cases are cortical-medullary involved type, 7 (53.8%) cases are cortex-medullary-pelvis involved type. 11 (84.6%) cases were nephritis type and 2 (15.4%) cases were mass type. The lesions appeared solid or complex solid and cystic on CT and MRI. The parenchymal part of 13 CDC tumors showed isodensity or slightly higher density on unenhanced CT scan. Two patients with PET/CT showed increased radioactivity intake. Evidence of intra-abdominal metastatic disease was present on CT in 9 (69.2%) cases.

Conclusions: The Collecting (Bellini) duct carcinoma has its certain imaging characteristics which were different from the other renal cell carcinoma. A renal tumor should be considered as CDC when it locates in the junction zone of the renal cortex and medulla, with unclear border, slight enhancement and metastases in early stage. PET/CT can greatly enrich the key information of diagnosis, surgery and treatment options, which provide significant help to the clinic.

Background

Collective duct carcinoma (CDC) is a highly malignant kidney tumor which is rare in clinical, accounting for 1% to 2% of renal cell carcinoma. Most patients have distant metastasis at initial diagnosis[1-2]. Unlike common renal cell carcinoma (RCC), CDC is considered to be derived from the renal medulla of Bellini tube. The biological behavior, morphological and functional manifestations of CDC have unique characteristics and significant differences between other types of renal cell carcinomas[3,11-13]. Therefore, based on reviewing the literatures, we retrospectively analyzed the image findings of 13 cases of renal collecting duct carcinoma in order to improve the understanding of the imaging features of the disease.

Methods

General Information

A total of 13 cases of renal collecting ducts confirmed by surgical pathology from January 2007 to December 2019 were collected, including 10 males and 3 females, aged from 46-78 years old with an average age of 64.23±10.74 years old. All 13 patients underwent CT scan, 8 of whom underwent contrast-enhanced multiphase CT scan, 2 underwent PET/CT scan and 1 underwent MRCP examination.

Check methods

The technique varied somewhat because of the retrospective nature of the study. The CT was subjected to a Philips Brilliance 256-slice CT with a horizontal transposition and enhanced scan. The scanning conditions are 120kV, 250mA, scan matrix 512×512, pitch 1.0, layer thickness 5mm, interval 5-10mm, and part of the layers are reconstructed by thin layer of 1~2mm. Enhanced scanning uses non-ionic contrast agent (300mgI / ml), the dose of 1.5 ~ 2.0ml / kg, high pressure syringe intravenous injection of the anterior elbow, the flow rate is 3ml / s, the cortical phase begins 25s after the injection of contrast agent. The substantial period starts from 70s and the renal pelvic phase begins at 150s.

MRI was GE Signa HDx 1.5T superconducting magnetic resonance instrument with body phased array coil. We used fast spin echo (FSE) T2WI, chemical displacement fat suppression, no pressurized Fiesta sequence scan with a layer thickness of 6 mm and a pitch of 2 mm, TR/TE18300/910, observation field 38cm, reconstruction matrix 256×192, single-slice scanning time 2s.

^{18}F-FDG PET/CT check method: Using the US GE Discovery PET / CT Elite scanner, ^{18}F-FDG radiochemical purity >95%, fasting 6h or more before the examination, fasting blood glucose <11.0mmol / l, ^{18}F-FDG dose is 5.55~7.4MBq/kg. CT image was collected after 60 minutes of intravenous rest, the scanning parameters were 120~140KV, the tube current was 200~300mA, the layer thickness was 3.75mm, and then the emission scan was performed. The examination range was from the head to the middle part of the femur. Attenuation correction is performed by CT. And all of the obtained PET/CT data is reconstructed using an iterative reconstruction technique. The workstation (Xeleris) is used to display, analyze and measure the SUVmax of the primary tumor.

Analysis methods

Two senior radiologists with 22 and 23 years of experience read the imaging together and evaluated the location, contour, size, internal structure, enhancement, neovascularity, calcification, surrounding structure of the lesions, infiltration, metastasis and PET/CT findings. Lesion size was determined by measuring the maximal diameter of each lesion on axial images. According to the involving part of collecting ductal carcinoma, it is divided into simple medullary involved type, cortico-medullary involved type and cortico-medullary-pelvis involved type[28]. Both readers were blinded to all clinical and pathologic findings. The pattern of enhancement was classified as homogeneous if the lesion enhanced in a uniform manner or heterogeneous if several areas within the lesion enhanced more than others. Neovascularity was defined as the presence of two or more unnamed large (>2 mm) vessels in the perinephric space

adjacent to the mass[27]. If there was any disagreement between the two readers regarding any of the features, a discussion was conducted between the two readers until a consensus was reached. Thus, a consensus was reached for all features in all patients. Finally we compared the surgical and pathological results and summed up its characteristics.

We divided the lesions into nephritis type and mass type according to the morphology of the tumors. Nephritis-type lesions are characterized by diffuse or localized changes in the kidney. Mostly are mixed density with major low density. The renal medulla is partially blurred, unclear, and the kidney outline is not changed. The mass lesions are intrarenal masses. Unlike typical common carcinoma, it tends to be more clearly defined and the mass protrudes from the outline of the kidney[19].

Results

Clinical Findings

Among the 13 patients, 10 were male and 3 were female, aged from 46 to 78 years old, with an average age of 64.23±10.74 years old. Only one patient was younger than 50 years old. The main clinical manifestations including 11 (84.6%) cases of gross hematuria, 6 (46.2%) cases of low back pain or lumbar discomfort, one of them suspecting of renal tuberculosis was admitted to hospital (Table 1). This group of 13 cases of CDC were all single disease, including 8 (61.5%) cases of left kidney and 5 (38.5%) cases of right kidney.

Table 1 Clinical data and major imaging findings of renal collecting ductal carcinoma

Gender	Age(Y)	Clinical Manifestations	Size(cm)	Site	Involved Part	Morphology	Composition	Border	Calcification	Metastasis	Examinatio
Male	61	Gross Hematuria, Low Back Flank Pain	9.14	Left	Cortex-Medullary	Nephritis Type	Solid-Cystic	unclear	No	Yes	Enhanced CT
Male	67	Irritating dry cough, bloodshot, low fever, fatigue and night sweats	5.95	Left	Cortex-Medullary	Nephritis Type	Solid	unclear	No	No	Enhanced CT
Female	74	Gross Hematuria	12.10	Left	Cortex-Medullary-Pelvis	Nephritis Type	Solid	unclear	No	Yes	Enhanced CT PET/CT
Female	51	Gross Hematuria	7.00	Left	Cortex-Medullary-Pelvis	Nephritis Type	Solid	unclear	No	Yes	Enhanced CT
Male	76	Gross Hematuria, Low Back Flank Pain	7.09	Right	Cortex-Medullary-Pelvis	Nephritis Type	Solid-Cystic	unclear	No	Yes	Enhanced CT
Male	68	Gross Hematuria	7.32	Left	Cortex-Medullary	Mass Type	Solid-Cystic	unclear	No	Yes	Enhanced CT
Male	74	Gross Hematuria	8.00	Right	Cortex-Medullary	Nephritis Type	Solid	unclear	No	No	Enhanced CT
Male	60	Gross Hematuria, Low Back Flank Pain	8.00	Left	Cortex-Medullary-Pelvis	Nephritis Type	Solid	unclear	Yes	Yes	Enhanced CT
Male	73	Gross Hematuria	6.08	Right	Cortex-Medullary-Pelvis	Nephritis Type	Solid	unclear	No	No	Non-enhanced CT
Male	78	Gross Hematuria、Dysuria	5.12	Left	Cortex-Medullary-Pelvis	Nephritis Type	Solid	unclear	No	Yes	Non-enhanced CT MRCP
Male	53	Gross Hematuria, Low Back Flank Pain	10.00	Left	Cortex-Medullary-Pelvis	Nephritis Type	Solid	unclear	Yes	Yes	PET/CT
Male	54	Gross Hematuria, Low Back Flank Pain with Frequent Urination, Urgency	12.10	Right	Cortex-Medullary	Mass Type	Solid-Cystic	clear	No	No	Non-enhanced CT
Female	46	Low Back Flank Pain	12.40	Right	Cortex-Medullary	Nephritis Type	Solid-Cystic	unclear	No	Yes	Non-enhanced CT

Site and Border

The location of the tumor was different, including 5 (38.5%) cases involving the whole kidney, 5 (38.5%) cases involving the upper pole of the kidney, and 3 (23.1%) cases involving the lower. In this group of cases, 6 (46.2%) cases are cortical-medullary involved type, 7 (53.8%) cases are cortex-medullary-pelvis involved type. There is no simple medullary involved type (Table 1). The central part of the tumor is mostly located in the junction zone of the renal cortex and medulla. And the tumors diffuse from the cortex and medulla to the inner and outer sides. The medial and renal pelvis structures are unclear. The renal pelvis and renal hilum structure is visibly damaged (Fig. 1-A).

The borders of renal collecting duct carcinoma are mostly unclear. In this group of cases, the edge of 12 (92.3%) lesions is unclear, and no obvious signs of capsules can be seen. Only one case of mass type can be seen with obvious boundary (Table 1). We suspect that the boundary is the compressed renal cortex (Fig. 1-B).

Morphology and Size

Maximal tumor diameter ranged from 5.12 to 12.40 cm (mean diameter, 8.48 ± 2.48cm) , 4 (30.8%) cases measured greater than 10 cm, 9 (69.2%) cases measured less than 10 cm (Table 1).

In this group, 11 (84.6%) cases were nephritis type and 2 (15.4%) cases were mass type (Table 1). There were no significant increases in renal volume in 3 (23.1%) cases of nephritis type, 8 (61.5%) cases of nephritis type had a slight increase in kidney volume, 6 (46.2%) cases had a clear outline of the kidney (Fig. 1-A), and 2 (15.4%) cases had a lobular change in renal contour. Two cases of tumor-like kidneys showed a mass-like enlargement and a marked change in kidney morphology (Fig. 1-B).

CT and MRI Characteristics

The lesions appeared solid or complex solid and cystic on CT. The unenhanced CT showed major solidity (Fig.2-A). 8 (61.5%) cases of small cystic component that represented areas of necrosis. The solid parts of the tumor appear as soft-tissue density which is higher than normal renal parenchyma. The other remaining 5 (38.5%) were complex solid and cystic lesions (Fig. 2-B) , all of which were single cysts. The density was uneven in 12 (92.3%) cases. Multiple sand-like calcifications were seen in one lesion. In this group, 7 (53.8%) cases of cortical-medullary-pelvis involved type and 2 (15.4%) cases of cortex-medullary involved type showed different degrees of caliectasis. 4 (30.8%) cases of cortex-medullary involved type did not show caliectasis (Table 1). MRI images on T2WI showed the affected side hypointense or isointense to the contralateral renal parenchyma (Fig. 3 A-B). The cystic area appeared high signal on T2WI.

Enhancement characteristics

Compared with the adjacent normal renal parenchyma, the parenchymal part of 13 CDC tumors showed isodensity or slightly higher density on unenhanced CT scan. CT value arranged from 37.00 to 41.55 HU and the average value was about 38.71±1.53HU (the average CT value of the same layer of renal cortex was 38.17±2.78HU). There were 8 (61.5%) cases showed the solid part of the tumor uneven patchy slight (7 cases, 35.8%) to moderate (1 case, 7.7%) enhancement on enhanced CT (Fig. 4). There was no enhancement in the cystic and necrotic areas. The mean CT value was about 61.61±5.81HU in the cortical phase (the average CT value of the renal parenchyma was about 170.85±56.48HU). The net increase CT value in cortical phase was 23.50HU. The medullary phase was about 68.47±10.64HU (the average CT value of the renal parenchyma was about 137.44±34.38HU). The excretion period showed nine tumors low attenuation compared with that of normal parenchyma. The excretion period was about 65.47±5.60HU (the average CT value of renal parenchyma was about 120.25±17.91HU). The CT value increased from 10.00 to 39.04 HU with an average of 26.90 ± 8.32 HU from the unenhanced CT to the medulla period enhanced CT (Table 2) .

Table 2 Characteristics of unenhanced and enhanced renal collecting ductal carcinoma

NECT Value（HU）	Cortical Phase CT Value（HU）	Net Increase CT Value in Cortical Phase（HU）	Medullary Phase CT Value（HU）	Net Increase CT Value in Medullary Phase（HU）	Excretion Period CT Value（HU）
37.00	52.00	15.00	72.76	35.76	68.13
37.50	57.83	20.33	58.48	20.98	63.97
37.00	60.00	23.00	47.00	10.00	55.00
37.80	60.76	22.96	76.84	39.04	67.45
37.82	61.32	23.50	70.86	33.04	62.92
37.34	62.80	25.46	69.32	31.98	64.22
40.87	66.56	25.69	79.03	38.16	67.41
39.79	71.62	31.83	73.47	33.68	74.69
41.55	—	—	—	—	—
38.08	—	—	—	—	—
40.21	—	—	—	—	—
38.76	—	—	—	—	—
39.52	—	—	—	—	—

The tumor enlargement artery and the new tumor blood vessels were not found in CTA reconstruction of 8 (61.5%) cases of CDC. There are 7 (53.8%) cases showed renal artery branches within tumors obviously attenuate or sparse (Fig. 5). Obvious abnormal venous drainage were not seen in all the cases.

PET/CT findings

Two patients with PET/CT showed increased renal radioactivity intake (Fig. 6 A-C). The maximum SUV values were 14.9 and 14.3 respectively (the maximum SUV values of normal renal parenchyma were 3.6 and 2.9 respectively). CT showed the corresponding sites as isodensity masses. One case of CT scan showed unclear lesion. However, PET/CT showed significant metabolic activity with extensive systemic metastases, including mediastinal, retroperitoneal lymph node metastasis, homolateral adrenal gland, bilateral lungs, bilateral pleura, right ribs, left scapula, and right pubic symphysis.

Local invasion and distant metastasis

Evidence of intra-abdominal metastatic disease was present on CT in 9 of 13 (69.23%) cases (Table 1). Perirenal infiltration of renal collecting ductal carcinoma is common. In this group, 12 (92.3%) cases of blur perirenal fat space or prerenal fascia thickening can be observed. 9 (69.2%) cases showed direct invasion of peritoneal and lymphatic metastasis (Fig. 7 A-B). Seven of them wrapped the renal artery and caused renal artery stenosis (Fig. 5 A-B). Adrenal gland involvement can be observed in 2 (15.4%) cases, 1 case as left side, 1 case as bilateral sides. 1 (7.7%) case showed inferior vena cava involved. 3

(23.1%) cases of bilateral lung metastases. 1 (7.7%) case of bilateral pleura metastases. One (7.7%) case of brain metastases and one (7.7%) case of bone metastases (right ribs, right pubic symphysis, and left scapula).

Discussion

Overview

In 1976, Mancilla Jimenez et al. first reported that some papillary renal cell carcinoma originated from the collecting duct. Fleming and Lewi described 6 cases of CDC and presented diagnostic criteria to recognize it as a unique pathologicalsubtype of RCC[14]. It was listed as one of the major subtypes of renal cell carcinoma in both the 2002 and 2006 WHO classifications. The key point of pathological diagnosis is the nail-like cells are covered on the inner surface of the papillary gland arranged on the tumor cells. The tumor interstitial inflammatory fibrosis and collagen secretion are obvious and the tumor tissue is dense. The pathological examination results of this group of cases basically conform to these characteristics (Figure 8 A-D).

A wide patient age range exists, with a mean age at diagnosis of 64 years and a 3:1 male predominance. Although it is similar to the series of reports[8,9], this demographic profile also applies to renal cell carcinoma in general and is therefore not a useful discriminator. The clinical manifestations of the patient are not specific compared to any other renal cell carcinomas and may have gross hematuria and waist and abdomen pain, abdominal fullness, and sometimes palpable mass[6]. 11 (84.6%) cases had gross hematuria, and 6 (46.2%) had low back pain or lumbar discomfort. One of the patients had no clinical manifestations of urinary disease with low fever and night sweats and admitted to hospital for suspected tuberculosis.

Site and Border

CDC has the following pathological features. The initial site of the tumor is in the renal medulla, which is grayish white or light yellow. The texture is more tough than the clear cell carcinoma. The renal interstitial is used as a scaffold for tumor cells to diffuse and infiltrate along the collecting duct to the renal pelvis and renal cortex[9]. Therefore, most of the tumors occur in the medulla and infiltrate into the cortex and renal pelvis. There is no clear junction with normal kidney tissue. The borders are irregular and most of the kidney tumors have an outward expansive growth pattern from the center. Normal renal parenchyma is displaced and/or local kidney contour bulged and the formation of a pseudocapsule[17,19]. Jonathan RY et al. found that sarcomatoid RCCs and collecting duct carcinoma were both more likely than common RCC subtypes and benign RCC mimics to have an infiltrative spread pattern and an irregular contour. When used to discriminate sarcomatoid RCC and collecting duct carcinoma from other solid renal masses, an infiltrative spread pattern had a specificity of 93% (287/308) and sensitivity of 82% (9/11), while an irregular contour had specificity of 98% (303/308) and sensitivity of 64% (7/11)[26].

According to the infiltration site of CDC, it can be divided into medulla type, cortex-medulla type and cortex-medullary-pelvis type. There was no simple medullary type of this group of patients. The masses were mostly located in the cortex-medulla type (6 cases, 46.2%) and the cortex-medullary-pelvis type (7 cases, 53.8%) . This feature is different from the common renal clear cell carcinoma derived from cortical renal tubules[28]. The latter is centered on the renal cortex and invaded to the medulla or extrarenal. There is no uniformity and clear boundaries between uniformly strengthened normal kidney tissue and tumors centered on the cortex-medullary-pelvis. The tumor can rapidly grow toward the renal pelvis and cortex and destroy the renal pelvis and renal hilum structure, even severely involve the upper ureter. Thus, assessing for the presence of an infiltrative spread pattern and an irregular contour can provide a simple, noninvasive means of discriminating collecting duct carcinoma from other solid renal masses with a relatively high specificity, sensitivity, and negative predictive value[26].

Morphology and Size

The morphology of tumors is closely related to the biological behavior and growth pattern of tumors[17]. Despite its medullary derivation, almost all tumors exhibit focal cortical extension, and perinephric extension is also common[4]. It has been mentioned that the growth mode of CDC tumors is spread along the collecting duct with invasive growth and there is more fibrous tissue hyperplasia in tumor stroma[5,8]. Therefore, most of CDC are not as sharp as the other tumors in the kidney[28]. The tumors have diffuse enlargement based on the kidney contour or a certain kidney segment without clear boundaries, capsules or pseudocapsule. This characteristic can be observed in 12 of the 13 cases (92.3%) in our group. There are also 2 cases of mass-type in this group. In one case, the inflammatory fibrous tissue proliferation of the tumor interstitial of CDC is not significant. The tumor outline is bounded by the tumor cell aggregation area. Therefore, we believe that the morphology of CDC tumors is related to the degree of tumor interstitial fibrous tissue hyperplasia. The more significant interstitial fibrosis is, the less clear the tumor outline and vice versa. According to the morphological characteristics of the tumor, it is helpful to distinguish it from other kidney tumors.

The diameter of the tumors ranged from 5.12 to 12.40 cm (mean diameter, 8.48 ± 2.48cm) , 4 cases were greater than 10 cm. In general, the size of CDC is often relatively large. A medullary origin can be difficult to appreciate with large tumors[19]. Fukuya et al. described the CT findings of small tumors, all measuring between 3 and 4.5cm. These lesions were all centered in the renal medulla, four of five protruded in the central sinus, and none showed exophytic growth but, rather, preserved the reniform contour in all cases[30].

CT density and MRI signal

The originating organ of CDC is water-rich kidney tissue. The tumor stroma has more fibrous tissue hyperplasia and collagenation. So when compared with normal tumor tissue adjacent to the tumor, the tumor parenchyma show relatively high density, which is the overall feature of this group of CDC tumors in non-enhanced CT. This is different from renal cell carcinoma origining from renal cortex. CDC has obvious interstitial reaction. The interstitial is dense or the collagen secretion is large. Most of which are inflammatory fibroblastic tissue hyperplasia and rich in fibrous tissue components. It is an important basis for pathological diagnosis and appear as low signal on magnetic resonance T2WI.

The MR examinations reported by Pickhardt et al. (4 cases in total) showed that the parenchymal components of all 4 tumors showed equal signals on T1WI[19]. 1 case of tumor with multiple cystic components, each cyst showed a low to high T1 signal (including water, fat, bleeding and other signals). On T2WI, the parenchymal components of all 4 tumors were lower than normal renal parenchyma. There is no low signal on the edge of tumor indicating the presence of a pseudo-envelope observed on MRI[19]. In this group, 1 case of MRI showed that the tumor parenchyma was low signal on T2W1. The cystic necrosis area was high and low mixed signal on T2WI, which was unclear with the surrounding normal renal parenchyma. There was no obvious ring-shaped low T2WI signal-like pseudo-envelope.

The incidence of calcification in CDC tumors is probably due to more fibrous tissue in the tumor stroma and calcium salts are easy to deposit in fibrous tissue. However, only 2 (15.4%) cases of this group of data found calcification. In contrast to conventional RCCs, calcification was also observed in only one case in Seong KY's report[17]. Compared with the normal renal parenchyma which is rich in water, the tumor tissue is denser and the interstitium is rich in inflammatory fibrous tissue hyperplasia. Therefore, the tumor parenchyma is equal, high signal on T1WI and low signal on T2WI. Kato et al. described the signal intensity of CDC at T2-weighted imaging as isointense or hypointense, which was thought to be due to haemosiderin deposition[35]. Larger clear cell renal cell carcinomas tend to have a heterogeneous hyperintense signal on T2-weighted imaging, differentiating it from CDC.

Some liquid components can be seen as low-density areas in tumors. The shape is very irregular and the boundary is unclear. It is like the shape of a map or a lake, which is different from the necrotic morphology of common tumors. Combined with pathological results, we think these diffuse patchy low-density lesion should be based on the collagen denaturation zone. There is still a cystic lesion of cystic solid tumor in this group as a true cyst, which is a rare sign of CDC tumor. In the existing literature, only one of 17 cases of CDC reported by Perry is cystic CDC[19]. The inner wall is covered with true epithelium, and its pathological mechanism remains to be further studied. When the essential components and cystic components coexist, careful analysis of the characteristics of the essential part is conducive to diagnosis and differential diagnosis.

Enhancement characteristics

The results of this group of patients show that the vast majority of CDC tumors are hypovascular. Most of the CDC tumors in the dynamic enhanced scan show relatively low density in the renal cortex and medulla. The parenchymal part of the mass is uneven lightly-moderately enhanced by marginal in cortical or medullary phase (intracapsular papillary can also be strengthened) and lower than the surrounding renal parenchyma. The medullary phase showed uneven and mild delayed enhancement. The degree of enhancement was still lower than that of the renal parenchyma, which is consistent with the results of another group of Chinese study[33]. This enhancement type is different from the blood-rich clear cell renal cell carcinoma, renal medullary carcinoma, renal angiomyolipoma and renal angioma[34]. Seong KY et al[17]. also found that unlike in the case of the more common conventional RCC, contrast-enhanced CT scans of the CDCs usually demonstrated weak (69%) and heterogeneous enhancement (85%). This enhanced feature is still different from renal clear cell carcinoma, which is significantly enhanced in cortex phase, its density value quickly reaches its peak and decreases significantly during the medullary phase. This enhanced pattern of CDC tumors also contributes to the identification of renal clear cell carcinoma. Fujimoto et al. analyzed the enhancement pattern of renal cell carcinomas greater than 5cm in diameter on contrast-enhanced helical CT. They reported that strong enhancement equal to the renal cortex was noted only in conventional renal carcinoma (75%)[31]. Jeong KK et al. reported that conventional renal carcinoma showed stronger enhancement than nonconventional renal carcinomas in both the corticomedullary and excretory phases, and the tumors that enhanced more than approximately 84HU in the corticomedullary phase and 44HU in the excretory phase were likely to be conventional renal carcinoma, while our data showed only 23.5HU increased in cortical phase[32].

CTA can show that the renal artery participates in blood supply and the distal branches are destroyed. The filling defect can be seen in renal vein and inferior vena cava. The tumor thrombus has an expanded shape and the degree of enhancement is similar to the central necrotic area and the hypovascular area. No tumor blood vessels were observed in the vicinity of the tumor and the original renal blood vessels were not thickened or significantly displaced. These characteristics indicate that CDC tumor cells do not produce angiogenic factors, and the original renal artery branches are rarely destroyed by tumor cells. The fibrous tissue in the tumor stroma will also compress the intratumoral vessels, which is different from the renal tubular cell carcinoma. The renal tubular cell carcinoma has hyperplasia of vessels and in spherical shape with tumors.

PET/CT findings

Most common renal cell carcinomas have low FDG metabolism and are similar to normal renal parenchyma, ^{18}F-FDG PET has certain limitations in the detection and diagnosis of common renal cancer[20]. Due to renal collecting duct cancer is rare, there is not much literature on PET performance. Ye et al reported a case of collecting duct carcinoma with a maximum diameter of 4.6 cm in the right kidney. The SUVmax of PET was 7.0[21]. Two patients in our group underwent PET/CT examination, and the primary lesions were highly metabolized, with SUVmax of 14.9 and 14.3, respectively. Moreover, one of the PET/CT images showed higher metabolism in lymph nodes, lungs, pleura and multiple bone metastases, which was consistent with HU and other studies[22]. Compared with other common renal cancer pathological types (such as clear cell carcinoma), collecting duct carcinoma may be characterized by high invasiveness and poor prognosis, often showing high FDG uptake. ^{18}F-FDG PET/CT has obvious advantages in the judgment of renal tumor metastases. Besne I and other studies have shown that the 5-year survival rate of distant metastasis of urinary tumors is 0%-20%. However, if the isolated metastases are resected, the 5-year survival rate can reach 25%-50%[23]. Therefore, early detection of metastases is essential. Safaei et al reported that the sensitivity and specificity of PET for detecting renal cell carcinoma metastases were 87% and 100%, respectively[24]. Majhail et al studied biopsy or surgical resection of 36 metastatic lesions in 24 patients with renal cell carcinoma. The results showed that the specificity and positive predictive value of ^{18}F-FDG PET/CT for distant metastasis were 100%[25]. But this group of the high-metabolism lymph nodes revealed by PET/CT showed no metastasis after surgical resection, which proved that the diagnosis of lymph node metastasis by PET/CT remains to be discussed.

Local invasion and distant metastasis

CDC cancer has high malignancy, strong invasiveness and early metastasis. This feature has become a consensus[5,7,10,15-16,18]. The incidence of extracranial metastasis of CDC tumor in this group further confirms the characteristics of early metastasis of CDC. The incidence of metastasis reached 69%. The rapid metastatic spread and aggressiveness of the CDC may be due to its central or perihilar location[29]. The tumor has the characteristics of infiltration into the kidney and local lymph node metastasis and distant metastasis. Most patients have lymph nodes enlargement and distant organs metastasis. Among them, lymph node metastasis accounts for 80%, lung and adrenal metastasis accounts for 25%, and the liver metastasis accounted for 20%. The prognosis was extremely poor, the patients died within 2 years of onset. In this series, 9 (69.2%) cases had lymphatic metastasis, 3 (23.1%) cases had bilateral lung metastasis, 2 (15.4%) cases had adrenal gland involvement, 1 (7.7%) case had inferior vena cava involvement, 1 (7.7%) case had bilateral pleural metastasis, 1 (7.7%) case had brain metastasis, 1 (7.7%) case had bone metastases (including the right rib, pubis and left side scapula). This is due to its high degree of malignancy and invasive biological characteristics.

There are some limitations to our study. The main limitation is that the number of CDCs was too small for the analysis of CT and histopathologic findings to be significant. Future study with a larger number of cases is necessary.

Conclusion

CDC has the worst prognosis as most patients develop metastases. Early diagnosis is essential and may increase patient survival. According to the biological characteristics and pathological structure of CDC, comprehensive CT and MRI examinations, dynamic enhancement of performance by CT and MRI combined with multi-parameter observation and post-processing reconstruction show the characteristics of the lesion and the identification of other kidney lesions is important. The examination of PET/CT can greatly enrich the key information of surgery and treatment options.

Abbreviations

CDC: Collective duct carcinoma; RCC: renal cell carcinoma; CT: Computed tomograghy; PET/CT: Positron Emission Tomography Computed Tomography; MRCP: Cholangiopancreatography, Magnetic Resonance; ^{18}F-FDG: ^{18}F-fluorodeoxyglucose; SUV: Standardized Uptake Value

Declarations

Ethics approval and consent to participate

Ethics approval was obtained from Institutional Review Board of the First Affiliated Hospital of Harbin Medical University. The study is a retrospective study involving human data that has already been collected and did not require additional recruitment of human subjects, waiving the need for informed consent and done in accordance with the regulations set by the Institutional Review Board of the First Affiliated Hospital of Harbin Medical University.

Consent for publication

Not applicable.

Availability of data and materials

The datasets generated and analysed during the study are not publicly available due to patient privacy, but are available from the corresponding author upon reasonable request.

Competing interests

Not applicable.

Funding

Not applicable.

Authors' contributions

ZL and LL contributed equally to this paper. ZL and LL analysed the data and wrote the manuscript. HL collected the PET/CT data. HW and TC collected the CT and MRI data. QL collected the pathology data. MX obtained ethics approval for the study. LT and PF revised the manuscript. All authors read and approved the final manuscript.

Acknowledgements

Not applicable.

Author details

[1]Department of Radiology, the First Affiliated Hospital of Harbin Medical University, N0.23 Post Street, 150001 Heilongjiang, People's Republic of China. [2]Department of PET/CT, the Second Affiliated Hospital of Harbin Medical University, No.246 Xuefu Road, 150086 Heilongjiang, People's Republic of China.

[3]Department of Nuclear Medicine, Inner Mongolia Autonomous Region People's Hospital, No.20 Zhaowuda Road, 010017 Hohhot, People's Republic of China.
[4]Department of CT, the Second Affiliated Hospital of Harbin Medical University, No.246 Xuefu Road, 150086 Heilongjiang, People's Republic of China.
[5]Department of Pathology, the First Affiliated Hospital of Harbin Medical University, N0.23 Post Street, 150001 Heilongjiang, People's Republic of China.
[6]Department of Nuclear Medicine, the First Affiliated Hospital of Harbin Medical University, N0.23 Post Street, 150001 Heilongjiang, People's Republic of China.

References

1. Srigley JR, Moch H. Carcinoma of the collecting ducts of Bellini. In: Eble John N, Guido Sauter, Epstein Jonathan I, Sesterhenn Isabell A, eds. WHO Pathology and Genetics of Tumours of the Urinary System and Male Genital Organs. IARCPress Lyon; 2004.
2. Fleming S, Symes CE. The distribution of cytokeratin antigens in the kidney and in renal tumours. Histopathology. 1987;11:157–170.
3. Mostofifi FK, Sesterhenn IA, Sobin LH. Histological typing of kidney tumours. International Histologic Classifification of Tumors, No. 25. Geneva, WHO. 1981; 1981.
4. Genov, PP ; Kolev, NH ; Dunev, VR. A rare case of Bellini duct carcinoma. Urol Case Rep.2019 Jul ;25 :100899.
5. Kennedy SM, Merino MJ, Linehan WM, Roberts JR, Robertson CN, Neumann RD. Collecting duct carcinoma of the kidney. Hum Pathol. 1990;21:449–456.
6. A. Salako, T.A. Badmus, K.B. Badmos, et al. Renal cell carcinoma in a semi-urban population of south-western Nigeria. East African Medical Journal. 2017;94(1):37-43.
7. Bozo Kru Lin, Ivana Glumbic, Ante Reljic, Hrvoje Cupic, Boris Ruzic, Goran Stimac et al. Collecting duct carcinoma of the kidney: report of three cases. Acta Clinica Croat. 2000; 40: 21-5.
8. Matz LR, Latham BI, Fabian VA and Vivian JB: Collecting duct carcinoma of the kidney: a report of three cases and review of the literature. Pathology 1997,29: 354-359.
9. Srigley JR. The International society of urological pathology[ISUP] vancouver classification of Renal Neoplasia. Am J Surg Pathol. 2013; 37(10): 1469-89.
10. Salako AA, Badmus TA, Ikem I, et al. Bellini duct carcinoma of the kidney masquerading as an iliac bone tumour in an adult Nigerian.Pan Afr Med J.2017 ;27 :245
11. Wright JL, Risk MC, Hotaling J, et al. Effect of collecting duct histology on renal cell cancer outcome. J Urol 2009;182:2595-9.
12. Abern MR, Tsivian M, Polascik TJ, et al. Characteristics and outcomes of tumors arising from the distal nephron. Urology 2012;80:140-6.
13. May M, Ficarra V, Shariat SF, et al. Impact of clinical and histopathological parameters on disease specifc survival in patients with collecting duct renal cell carcinoma: Development of a disease specifc risk model. J Urol 2013;90:458-63.
14. Fleming S, Lewi HJ. Collecting duct carcinoma of the kidney. Histopathology 1986;10:1131.
15. Tokuda N, Naito S, Matsuzaki O, et al. Collecting duct (Bellini duct) renal cell carcinoma: A nation-wide survey in Japan. Japanese Society of Renal Cancer. J Urol 2006;176:40-3.
16. Karakiewicz PI, Trinh QD, Rioux–Leclercq N, et al. Collecting duct renal cell carcinoma: A matchedanalysis of 41 cases. Eur Urol 2007;52:1140-5.
17. Yoon SK, Nam KJ, Rha SH, et al. Collecting duct carcinoma of the kidney: CT and pathologic correlation.Eur J Radiol 2006;57:453-60.
18. Ciszewski, S; Jakimów, A; Smolska-Ciszewska, B. Collecting (Bellini) duct carcinoma: A clinical study of a rare tumour and review of the literature. Can Urol Assoc J.2015 ;9(9-10) :E589-93.
19. Pickhardt PJ, Siegel CL, McLarney JK. Collecting duct carcinoma of the kidney: are imaging findings suggestive of the diagnosis? AJR Am J Roentgenol 2001;176:627-33.
20. Zukotynski K, Lewis A, O'Regan K, et al. PET/CT and renal pathology:a blind spot for radiologisits?Part1, primary pathology. AJR Am J Roentgenol. 2012;99:W163-167.
21. Ye XH, Chen LH, Wu HB, et al: 18F-FDG PET/CT evaluation of lymphoma with renal involvement: comparison with renal carcinoma. South Med J 2010;103(7):642-9.
22. Hu Y, Lu GM, Li K,et al.Collecting duct carcinoma of the kidney: Imaging observations of a rare tumor. Oncol Lett. 2014 Feb;7(2):519-524.
23. Besne I，Descombes C，Breton L，Effect of age and anatomical site on density of sensory innervation in human epidermis. Arch Dermatol. 2002;138(11):1445-1450。
24. Safaei A，Figlin R,Hoh CK,et al.The usefulness of F-18 deoxyglucose whole-body positron emission tomography(PET) for re-staging of renal cell cancer.Clin Nephrol,2002,57(1):56-62.
25. Majhail NS, Urbain JL, Albani JM, Kanvinde MH, Rice TW, Novick AC, et al. F-18 fluorodeoxyglucose positron emission tomography in the evaluation of distant metastases from renal cell carcinoma. J Clin Oncol.2003;21:3995-4000.
26. Jonathan RY, Jocelyn AY, Daniel AM, et al. Sarcomatoid Renal Cell Carcinoma and Collecting Duct Carcinoma Discrimination From Common Renal Cell Carcinoma Subtypes and Benign RCC Mimics on Multiphasic MDCT. Acad Radiol, 2017 Oct;24(10):1226-1232.
27. Zhang J, Lefkowitz RA, Ishill NM, et al. Solid renal cortical tumors: differentiation with CT. Radiology 2007; 244:494–504.
28. Shao B, Zhang YG, Gao JB, et al. The CT and MRI diagnosis of collecting tubules carcinoma of kidneys. J Radiol Practice. 2016 Oct;31(10):943-946.
29. Kuroda N, Toi M, Hirol M, et al. Review of collecting duct carcinoma with focus on clinical and pathobiological aspects. Histol Histopathol 2002;17:1329-34.
30. Fukuya T, Honda H, Goto K, et al. Computed tomo-graphic findings of Bellini duct carcinoma. J Comput Assist Tomogr 1996;20:399-403.

31. Fujimoto H, Wakao F, Moriyama N, et al. Alveolar architecture of clear cell renal carcinomas (< or = 5.0 cm) show high attenuation on dynamic CT scanning. Jpn J Clin Oncol 1999;29:198-203.
32. Jeong KK, Tae KKim, Han JA et al. Differentiation of Subtypes of Renal Cell Carcinoma on Helical CT Scans. AJR Am J Roentgenol. 2002 Jun;178(6):1499-506.
33. Zhu Q, Wu J, Wang Z et al. The MSCT and MRI findings of collecting duct carcinoma.Clin Radiol. 2013 Oct;68(10):1002-7.
34. Sauk SC, Hsu MS, Margolis DJ, et al. Clear cell renal cell carcinoma: multiphasic multidetector CT imaging features help predict genetic karyotypes. Radiology 2011;261:854-62.
35. Kato H, Kanematsu M, Yokoi S, et al. Renal cell carcinoma associated with Xp11.2 translocation / TFE3 gene fusion: radiological findings mimicking papillary subtype. J Magn Reson Imaging 2011;33:217-20.

Tables

Table 1 Clinical data of renal collecting ductal carcinoma

Clinical Manifestations	Size（cm）	Incidence Site	Involved Part	Morphology	Composition
Gross Hematuria，Dysuria	5.12	Left	Cortex-Medullary-Pelvis	Nephritis Type	Solid
Irritating dry cough, bloodshot, low fever, fatigue and night sweats	5.95	Left	Cortex-Medullary	Nephritis Type	Solid
Gross Hematuria	6.08	Right	Cortex-Medullary-Pelvis	Nephritis Type	Solid
Gross Hematuria	7	Left	Cortex-Medullary-Pelvis	Nephritis Type	Solid
Gross Hematuria，Low Back Flank Pain	7.09	Right	Cortex-Medullary-Pelvis	Nephritis Type	Solid-Cystic
Gross Hematuria	7.32	Left	Cortex-Medullary	Mass Type	Solid-Cystic
Gross Hematuria	8	Right	Cortex-Medullary	Nephritis Type	Solid
Gross Hematuria，Low Back Flank Pain	8	Left	Cortex-Medullary-Pelvis	Nephritis Type	Solid
Gross Hematuria，Low Back Flank Pain	9.14	Left	Cortex-Medullary	Nephritis Type	Solid-Cystic
Gross Hematuria，Low Back Flank Pain	10	Left	Cortex-Medullary-Pelvis	Nephritis Type	Solid
Gross Hematuria，Low Back Flank Pain with Frequent Urination, Urgency	12.1	Right	Cortex-Medullary	Mass Type	Solid-Cystic
Gross Hematuria	12.1	Left	Cortex-Medullary-Pelvis	Nephritis Type	Solid
Low Back Flank Pain	12.4	Right	Cortex-Medullary	Nephritis Type	Solid-Cystic

Table 2 Characteristics of unenhanced and enhanced renal collecting ductal carcinoma

NECT Value（HU）	Cortical Phase CT Value（HU）	Net Increase CT Value in Cortical Phase（HU）	Medullary Phase CT Value（HU）	Net Increase CT Value in Medullary Phase（HU）	Excretion Period CT Value（HU）
37.00	52.00	15.00	72.76	35.76	68.13
37.50	57.83	20.33	58.48	20.98	63.97
37.00	60.00	23.00	47.00	10.00	55.00
37.80	60.76	22.96	76.84	39.04	67.45
37.82	61.32	23.50	70.86	33.04	62.92
37.34	62.80	25.46	69.32	31.98	64.22
40.87	66.56	25.69	79.03	38.16	67.41
39.79	71.62	31.83	73.47	33.68	74.69
41.55	—	—	—	—	—
38.08	—	—	—	—	—
40.21	—	—	—	—	—
38.76	—	—	—	—	—
39.52	—	—	—	—	—

Figures

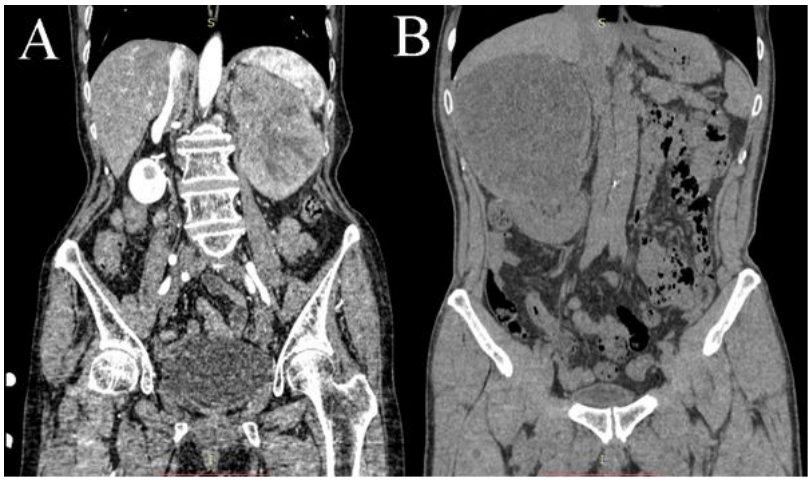

Figure 1

Case 13: Coronary unenhanced CT image a shows left kidney collecting ductal carcinoma. The tumor involves the renal cortex, medulla and renal pelvis. The boundary is unclear. Case 12: Coronary unenhanced CT image b shows right kidney mass-type collecting duct carcinoma. The tumor compresses the surrounding renal cortex and medulla. The boundary is obvious, which is considered as the compressed renal cortex.

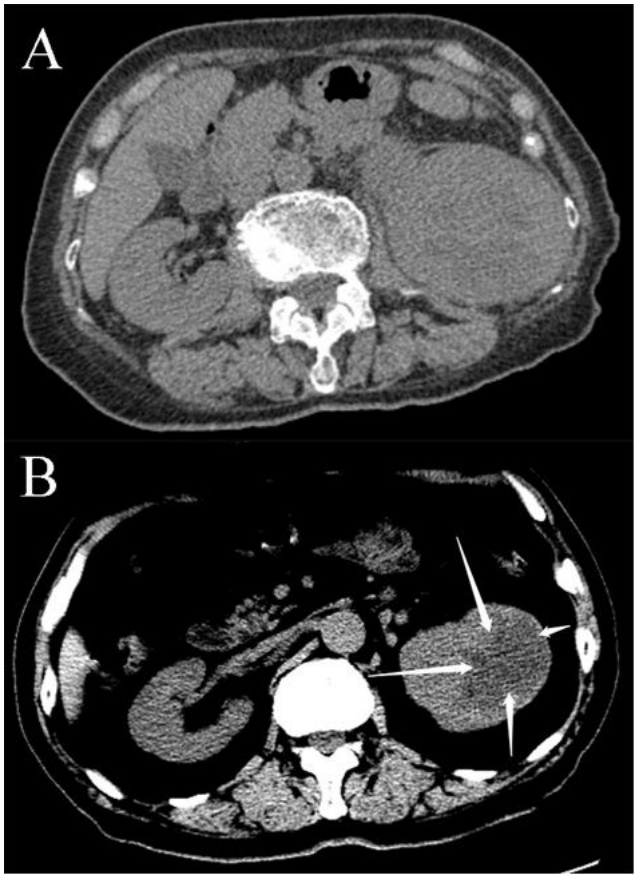

Figure 2

Case 3: Axial unenhanced CT image a shows a significant increase in the volume of the left kidney collecting ductal carcinoma. The left medulla is unclear. The lesions are mainly solid components. Case 6: Axial unenhanced CT image b shows mixed density in the left kidney. A clear cystic low-density lesion with a clear border (arrows).

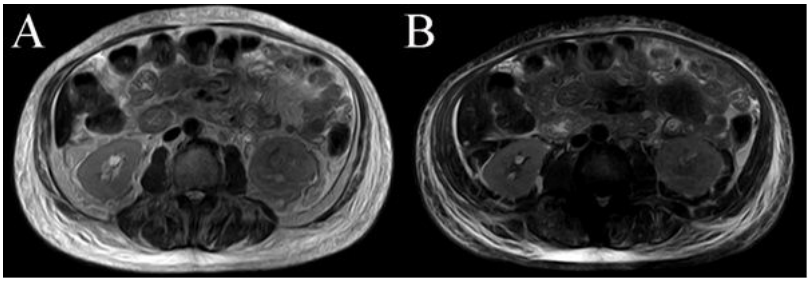

Figure 3

Case 10: Axial unenhanced T2WI image a shows that the left kidney collecting ductal carcinoma signal is lower than the normal renal parenchyma. The renal pelvis and renal medulla are unclear. Axial unenhanced fat-saturated T2WI image b shows slightly lower signal than normal renal parenchyma.

Figure 4

Case 5: Axial unenhanced/enhanced CT image of collecting ductal carcinoma shows that the right renal medulla unclear. The internal density is uneven with light-moderate delayed enhancement.

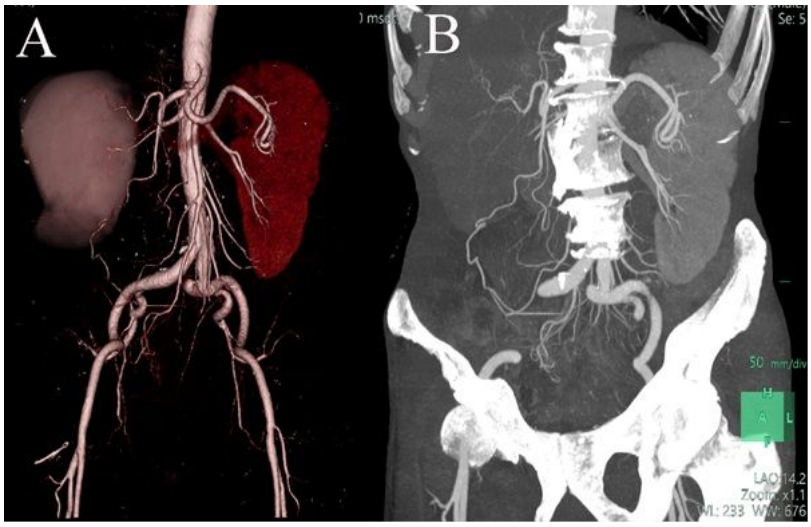

Figure 5

Case 5: Right kidney of collecting ductal carcinoma. Volume rendering images a and maximum intensity projection images b of arterial contrast-enhanced CT shows pressure of right renal artery.

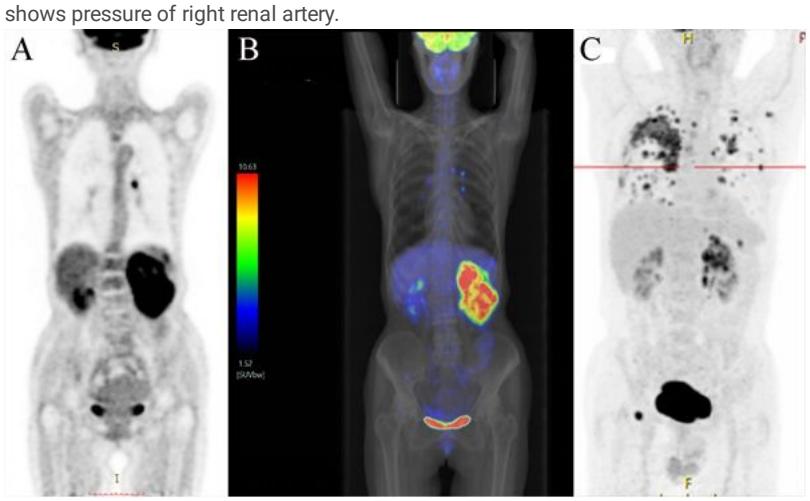

Figure 6

Case 11: PET/CT images of renal collecting duct carcinoma a shows significant concentration in the left kidney area with a maximum SUV of 14.9. PET/CT and simulated X-ray fusion images b showed significant concentration in the left kidney region with a maximum SUV of 14.9. Case 3: PET/CT image c shows increased metabolism of left renal collecting ductal carcinoma with extensive systemic metastases including mediastinal, retroperitoneal lymph node metastasis, homolateral adrenal gland, bilateral lungs, bilateral pleura, right ribs, left scapula and right side pubic symphysis.

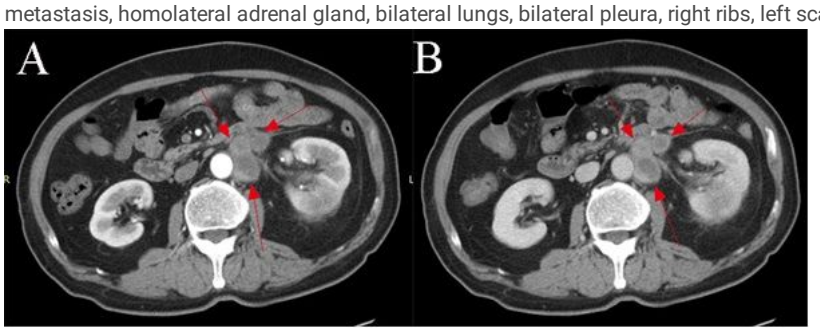

Figure 7

Case 6: Axial enhanced CT image a shows left renal collecting ductal carcinoma. axial arterial phase image shows multiple retroperitoneal enlarged lymph node with marginal mild enhancement (arrows). Axial delayed phase image b shows further strengthening which is similar to renal collecting ductal carcinoma (arrows).

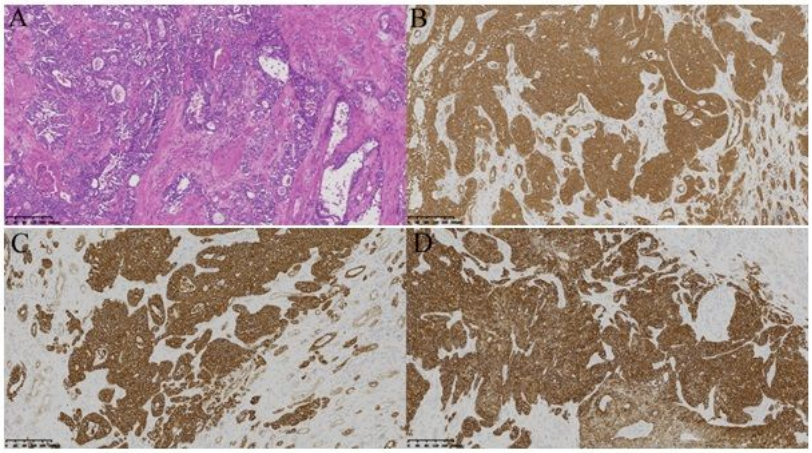

Figure 8

Case 1: The pathological images of CDC. a The tumor cells are cuboidal. The cytoplasm is eosinophilic or suspicion. The nucleus is large. The nucleolus is obvious and it is arranged in a small tubular or papillary shape, while the atypical shape is obvious. Immunohistochemistry shows b cam5.2(+), c CK(+), d 34βE12(+).